REVIEW

Electrochemical plasmonic sensors

Andreas B. Dahlin · Bernd Dielacher · Prayanka Rajendran · Kaori Sugihara ·
Takumi Sannomiya · Marcy Zenobi-Wong · Janos Vörös

Abstract The enormous progress of nanotechnology during the last decade has made it possible to fabricate a great variety of nanostructures. On the nanoscale, metals exhibit special electrical and optical properties, which can be utilized for novel applications. In particular, plasmonic sensors including both the established technique of surface plasmon resonance and more recent nanoplasmonic sensors, have recently attracted much attention. However, some of the simplest and most successful sensors, such as the glucose biosensor, are based on electrical readout. In this review we describe the implementation of electrochemistry with plasmonic nanostructures for combined electrical and optical signal transduction. We highlight results from different types of metallic nanostructures such as nanoparticles, nanowires, nanoholes or simply films of nanoscale thickness. We briefly give an overview of their optical properties and discuss implementation of electrochemical methods. In particular, we review studies on how electrochemical potentials influence the plasmon resonances in different nanostructures, as this type of fundamental understanding is necessary for successful combination of the methods. Although several combined platforms exist, many are not yet in use as sensors partly because of the complicated effects from electrochemical potentials on plasmon resonances. Yet, there are clearly promising aspects of these sensor combinations and we conclude this review by discussing the advantages of synchronized electrical and optical readout, illustrating the versatility of these technologies.

Introduction

Over a century ago, Paul Drude [1] described metals as plasmas of free electrons, forming a physical basis for their optical and electrical properties. Even today, this is usually how we understand metals, at least qualitatively. For several metals, the classic Drude model also provides quantitatively accurate results within optics and electronics as long as quantum effects can be disregarded, which typically is the case for length scales above 10 nm. Yet, in nanoscale (smaller than 1 μm) structures, several interesting optical and electrical phenomena occur, such as plasmon excitation by light and environmental influences on conductivity. Such effects are highly *surface sensitive*, i.e. they respond to changes in the environment that occur locally on the surface. This has led to the development of novel sensors and biosensors operating label-free [2], i.e. with the *analyte* in its native state and usually in real time. These sensors have no need for reporter elements such as fluorophores, radioactive labels or quantum dots, although such entities can be used in a secondary step to enhance the signal after

A. B. Dahlin (✉)
Bionanophotonics, Dept. of Applied Physics,
Chalmers University of Technology,
Fysikgränd 3,
41296 Göteborg, Sweden
e-mail: adahlin@chalmers.se

B. Dielacher · P. Rajendran · K. Sugihara · M. Zenobi-Wong ·
J. Vörös
Laboratory of Biosensors and Bioelectronics, Institute of
Biomedical Engineering, Swiss Federal Institute of Technology,
8092 Zurich, Switzerland

T. Sannomiya
Department of Metallurgy and Ceramics Science,
Tokyo Institute of Technology,
S8-6, 2-12-1 Ookayama, Meguro-ku,
Tokyo 152-8552, Japan
e-mail: sannomiya@mtl.titech.ac.jp

binding [3, 4]. The most successful emerging technologies are arguably those based on optical or electrical signal transduction. Optical and electrical techniques tend to be simple, robust and can easily be miniaturized in comparison with mechanical methods or less common approaches, such as thermal [5] or magnetic [6] sensors. Systems with mechanical signal transduction, such as the quartz crystal microbalance [7], surface acoustic waves [8] and cantilevers [9], are also aided by electrical and optical principles since piezoelectric movement is controlled by electronics and deflection is measured optically.

Most optical methods are refractometric, i.e. they respond to the refractive index (RI) changes caused by the analyte. They are in general based on either interferometry or excitation of an optical resonance [10], such as in surface plasmon resonance (SPR) [11]. SPR has long been the dominating technique for label-free biomolecular interaction analysis [12] providing a typical RI resolution of 10^{-7} and a limit of detection (LOD) down to 0.01 ng/cm^2 in terms of surface coverage [11]. Notably, the LOD in terms of analyte *concentration* will always be influenced by binding kinetics [13] for SPR and all other surface-sensitive techniques. In addition, most assays suffer from non-specific interactions in complex samples [14, 15], which puts high demands on the chemistry used for surface functionalization. Yet, in many applications of SPR the LOD in terms of concentration is comparable to or better than that in enzyme-linked immunosorbent assays [11].

During the last decade, nanoplasmonic (or "localized SPR") sensors based on various nanostructures (not just thin metal films) have become a popular research topic [16, 17]. It is suggested that such sensors are preferable over SPR in terms of miniaturization [18] and simplicity [19] (e.g. no prism or polarizer). Despite a lower sensitivity to RI changes, localized SPR sensors can provide comparable performance in refractometric detection owing to strongly confined fields [15, 20–22]. Recent studies suggest the sensitivity can be enhanced further by Fano resonances [23] or metamaterials [24]. There are also several interesting assays [25, 26] and distance measurements [27–29] in biological systems based on plasmonic coupling between plasmonic nanoparticles that are free in solution. Such particles have some advantages as labels since they do not bleach like fluorophores and have low toxicity [30]. Nanoplasmonic systems have also been proposed for spectral detection and *identification* through inelastic spectroscopy techniques such as surface-enhanced Raman scattering (SERS) [31].

Another way to move the free electrons in metals is by electrical control. Electrical sensing methods are often based on conductivity changes caused by field effects [32], usually in semiconductor nanowires [33]. Multiplexed detection of proteins in blood with a LOD in terms of concentration down to a few femtomoles per litre has been reported [34]. In contrast, voltammetry can be used to measure currents from oxidation or reduction of analytes [35]. In this case specificity can be achieved by using enzymes [36] (as in common glucose-sensing devices), redox cycling [37] (especially in small volumes) or fast scanning [38] (also in vivo). Another popular technique is electrochemical impedance spectroscopy (EIS) [39], which has a signal transduction that remains somewhat unclear [40]. Molecules on the surface can, for instance, either block charge transfer or induce changes in capacitance [41]. The technique has been employed with rather inconsistent methods, as will be discussed.

It is interesting to consider which metals are most suitable for electrical and optical sensing. Most bioanalytical systems utilizing electrical or optical detection contain gold as the active sensor surface mainly because it is a chemically stable metal which can be easily etched, e.g. by ion milling [42]. Gold also has a long electron mean free path, which results in relatively high conductivity and strong plasmon resonances. The latter effect is well known from the ruby red colour of colloidal gold, which for centuries has been used for staining glass [43]. The only metal that is closer to Drude-like ideal electron behaviour is silver, which has no interband transitions in the visible region [44] and higher conductivity [45] but its susceptibility to oxidation is a severe limitation. However, Anker et al. [19] and Haes and Van Duyne [46] have demonstrated successful use of silver nanoparticles as optical biosensors and the first SPR experiments were actually performed on silver films [47]. For copper, even worse oxidation issues apply [48] in combination with optical damping for visible wavelengths [44], although SPR coupling can be efficient [49] and as a bulk metal copper has good conductivity [45]. Platinum has the best oxidative stability but suffers from weak plasmon resonances [50].

Although there are reviews available covering the topics of electrical [35, 51] and in particular plasmonic [11, 12, 16, 17, 19] biosensors, the combination of these methods appears not to have been discussed so far. The topic of this review is the implementation of electrical readout in different types of plasmonic structures. Besides electrochemical SPR (ESPR) systems [36, 52–55] there are few existing combined systems actually in use *as sensors*. Yet, there are many studies on the implementation of electrochemistry with plasmonic nanoparticles and also some studies where other nanoplasmonic systems have been used. For one thing, it is clear that the plasmon resonances are influenced by applied electrochemical potentials. We will look more closely at such effects (summarized in Table 1) as they are critical for developing combined sensors. We give examples of how combined electrical and plasmonic readout has provided useful information, in particular for SPR. In the final section we

Table 1 Summary of the effects that may influence the optical spectrum of plasmon resonances (all types) when the metal is under the influence of electrochemical potentials. We assume the metal is not coated with molecules that change their optical properties and that there are no metal ions in solution. The effect is considered reversible if the optical spectrum returns to normal when the potential is released

Effect	Spectral changes	Reversible	Comments
Electron density changes	Resonance blue-shifts with higher electron density	Yes	A higher electron density increases the metal plasma frequency [64, 84]
Attracted free hydrated ions	Possibly a very small red shift	Yes	The electric double layer will increase the RI locally, but the effect is small [92].
Chemically bound ions	Usually resonance red shift and broadening	Depends on interaction	Formation of optically damping layers with high RI [92]. Reversible if the chemical interaction is reversible
Redox reactions	Red or blue shift	Yes	If a redox reaction occurs, there will be a signal from the difference in RI between the reactant and the product [54, 66]
Electrochemical crystallization	Blue shift and reduced peak width	No	Metal films that are not annealed may undergo crystal grain growth [42]. This strongly influences the plasmons [62]
Changes in metal shape and dimensions	Depends on structure	No	Metal dissolution at highly positive potentials or induced by halide ions [97]. Fine structural changes [90, 94]
Temperature changes	Depends on structure	Yes	The electrochemical activity could potentially heat the metal, which causes changes in the dielectric function [140]

RI refractive index

discuss more speculative advantages of plasmonic sensors with implemented electrochemistry.

Plasmonic systems with electrical control

Surface plasmon resonance

ESPR is an established method within academic research and has even been commercialized (e.g. Metrohm product Autolab ESPRIT). This is not surprising since SPR by itself is an established technique and the implementation of a basic electrochemical cell where the gold sensor chip acts as a working electrode is straightforward. Examples of ESPR sensors were reviewed by Zhang et al. [52] some time ago. Several studies have been performed on electropolymerization and doping processes in conductive multilayer molecular films [56–59] or layers containing chromophores [60]. The primary value of the sensor combination is that electron transfer reactions are quantified from the current, and the SPR readout provides the RI and possibly the thickness [36] of the layer. The relevance to sensing lies in the fact that polymeric films can cross conductivity thresholds or undergo strong optical changes upon redox reactions. For instance, this can be used to monitor activity of redox enzymes such as horseradish peroxidase [58].

Yet, ESPR experiments go even further back in time. Reflection measurements on metals with electrochemistry were presented by McIntyre [61] and the effect on surface plasmons was investigated more directly by Abeles et al. [53]. Tadjeddine et al. [62] experimentally determined a relation between surface plasmon excitation and applied voltage for silver [Ag (111) in 0.5 M $NaClO_4$]. In other words, the question how electrochemical potentials influence plasmon resonances has been considered for a long time. As shown in Table 1, it is clear that the spectral changes depend on multiple effects [63] even in the absence of electron transfer reactions [53]. Foley et al. [64] have discussed how the electron density of the metal, which is changed by an applied potential, changes the Drude plasma frequency, suggesting a linear relation between potential and SPR resonance angle shift. However, the ionic counterpart of the double-layer capacitor [65] was not considered and the electrons/holes were treated as delocalized through the metal film, although the charge depletion occurs in the top atomic layer [53].

Wang et al. [66] elegantly demonstrated how electrochemical reactions generate RI contrasts that can be visualized by SPR imaging (Fig. 1). In this case, the plasmonic readout essentially replaces the amperemeter in the system, with the advantage of providing imaging of gradients in the current density over the electrode surface [54]. The RI contrast is generated by molecular species which undergo charge transfer reactions and the signal is determined by the contrast
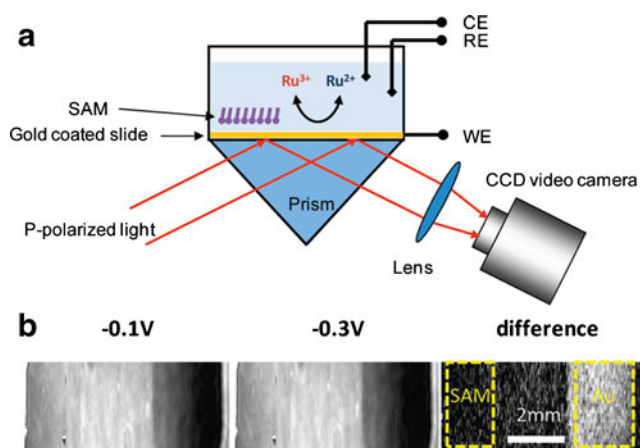
Fig. 1 The principle of plasmonic imaging of electrochemical currents using electrochemical surface plasmon resonance is shown in **a**. A redox reaction generates a local change in refractive index because of the reactants consumed and products generated (here ruthenium complexes). By imaging surface plasmon resonance, one can visualize where on the surface the reaction occurs (**b**). It is shown by comparing the signal from a clean gold surface how a self-assembled alkanethiol monolayer (*SAM*) can block charge transfer. *CE* counter electrode, *RE* reference electrode, *WE* working electrode. (Reprinted with permission from Wang et al. [66]. Copyright 2010 American Chemical Society)

in the RI between the oxidized and reduced states. In contrast to conventional voltammetry, the current measured through SPR is intrinsically normalized to the electrode area and the imaging SPR technique [67] determines the spatial resolution.

An ESPR sensor for glucose sensing based on conductive polymer films with the enzyme glucose oxidase incorporated was recently demonstrated by Baba et al. [36]. Common glucose sensors operate by monitoring the current from enzymatic oxidation at a maintained potential and this was possible also in this work. However, it was also demonstrated that the electrochromic properties of the surrounding polymer matrix may provide an RI contrast upon glucose oxidation which is high enough for the SPR readout to provide better signal to noise than ordinary chronoamperometry [36]. In other words, the current data are again replaced by the optical readout, but mainly for providing higher resolution in the detection.

Nanoparticles

Many types of gold nanoparticles can be synthesized by reduction of gold ions in solution [68–70]. On surfaces, colloidal patterns [71–76], electroplating [24] or imprinting [3] can give various particles over large areas, whereas serial electron beam lithography produces arbitrary shapes [23] but over smaller regions. It is important to note that the free-electron properties of the metal depend on the fabrication method since this influences crystal grain size [42]. Individual metal nanoparticles exhibit fully confined plas-

mon resonances at frequencies which depend on various particle properties, such as size [77], shape [78] and the Drude properties of the metal [42]. The RI of the local medium also influences the spectrum, which forms the basis for refractometric plasmonic detection [79]. In terms of pure electrochemical sensing, thin films of gold nanoparticles can be used as high-surface-area electrodes [80, 81].

To combine electrical and optical sensing for plasmonic nanoparticles, the first step is to understand how an electrochemical potential influences their optical properties. Pioneering work on nanoparticle plasmonics with implemented electrochemistry was reviewed by Mulvaney [82]. This demonstrated, among other things, how the plasmon resonance wavelength changed upon electron transfer to suspended particles. The primary physical explanation proposed was that electrons transferred to the particle change the free-electron density in the Drude model (Table 1), which increases the plasma frequency [83, 84]. Free particles can thus act as nanocapacitors with their charge monitored optically by the plasmon resonance wavelength [85]. (The relative change in electron density is equal to the relative change in wavelength squared.) An example of this type of optical monitoring of electrochemical processes is shown in Fig. 2.

Lately, it has become more common to have the particles bound to a conductive surface, which makes it much easier to exchange components in the liquid environment and control electrochemical potentials more quickly. Maintaining similar plasmonic properties of the particles requires a conductive yet transparent support such as indium tin oxide (ITO) [42, 86–94]. ITO is a doped semiconductor which has a charge carrier density that can be tuned [95] such that the material has decent conductivity, whereas the plasma frequency is low enough to make the material dielectric in the visible–near IR region and metallic (plasmonic) only relatively far into the IR region [95]. Further, the band gap is wider than the energy range of visible light.

For electrochemical–plasmonic sensing applications of nanoparticles, it is interesting to consider their stability and optical signals upon redox reactions with the metal. For one thing, ITO can be reduced at negative potentials [96], at least at −1.4 V against Ag/AgCl [88]. On the other hand, the metal will suffer from oxidative reactions and can be dissolved at positive potentials after forming complexes with halide ions [97]. The oxidation potential depends on particle size owing to the increased surface energy for smaller particles [98]. The optical response upon oxidation has been studied for colloidal gold on ITO and is in many cases reversible [87, 92]. Figure 3 shows an example of electrochemical chloridation of gold colloids (in NaCl) on ITO with synchronized spectroscopy. Hysteresis is clearly seen when the peak position or width is plotted against the applied potential, but the spectral changes remain reversible up to approximately +800 mV [92], i.e. no metal is
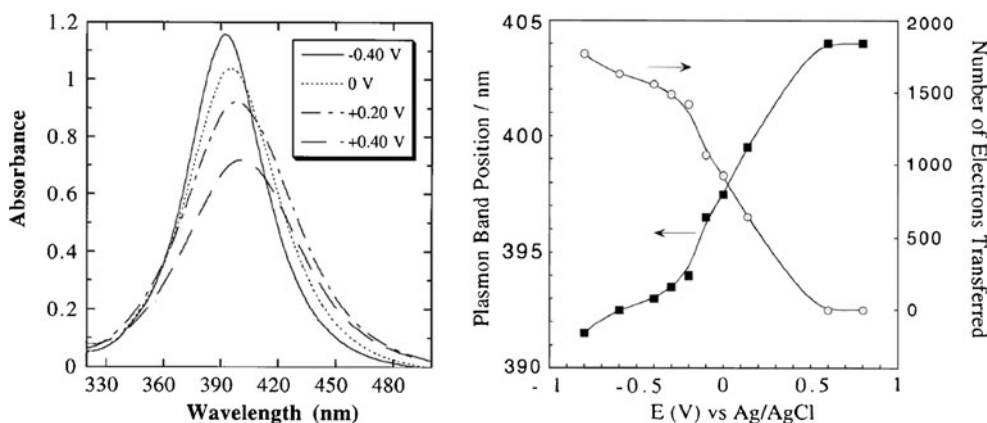
Fig. 2 Pioneering work on combined plasmonics and electrochemistry on 11-nm silver colloids suspended in a small liquid cell. The colloids were charged at a gold mesh electrode and the spectral data shown are those obtained upon establishment of equilibrium. The number of electrons transferred was calculated according to a model that relates resonance wavelength to electron density[84]. (Reprinted with permission from Ung et al. [84]. Copyright 1997 American Chemical Society)

dissolved. There are also reports about minor changes in the morphology of nanoparticles on ITO in response to electrochemical potentials. Preferential oxidation at the corners of triangular silver particles was observed by Zhang et al. [94], whereas Novo and Mulvaney [90] noted restructuring and faceting of gold nanorod edges.

It is clear from data such as those in Fig. 3 that chemical interactions with ions also strongly influence the optical response to electrochemical potentials, together with changes in electron density. Mulvaney [82] considered this effect and suggested that the resonance wavelength *shift* is associated with electron density changes, whereas the plasmon resonance
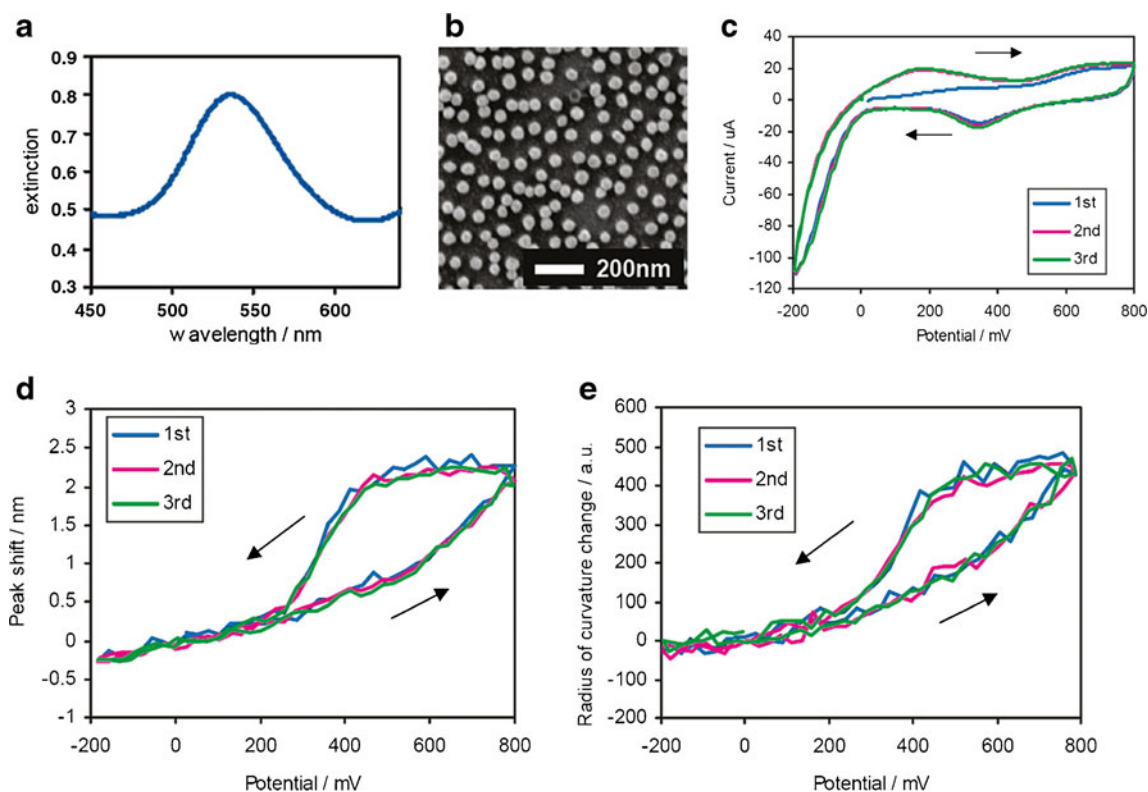
Fig. 3 Electrochemical formation of gold chloride on colloids supported by indium tin oxide monitored by cyclic voltammetry scans with synchronized spectroscopy. A spectrum of the structure in 100 mM NaCl is shown in **a** and an electron microscopy image is shown in **b**. The cyclic voltammetry current is shown in **c** for three cycles at 10 mV/s scan rate. In **d** and **e** the synchronized plasmonic response is shown in terms of peak shift and peak width, respectively. The experimental setup was similar to that shown in Fig. 5e. (Reprinted with permission from Sannomiya et al. [92]. Copyright 2009 American Chemical Society)

width is associated with chemically adsorbed ions, primarily halides. Still, it seems plausible that the formation of a layer with metal-ion complexes may also shift the resonance because of its high RI, as we suggested on the basis of modelling the full spectrum and measuring changes in peak position, width and magnitude [92]. Importantly, an early study by Gao and Weaver [99] with combined electrochemistry and SERS showed that Cl⁻, Br⁻ and I⁻ remain adsorbed to gold even at highly negative potentials (e.g. -600 mV against the saturated calomel electrode for Cl⁻). We have recently investigated the influence of chemical interactions with ions in further detail (A.B. Dahlin, R. Zahn and J. Vörös, unpublished work).

Since many questions still remain about the optical–electrical behaviour of nanoparticles, it is not so surprising that there are relatively few sensing applications of combined systems. Novo et al. [89] showed how optical detection can be used to measure catalytic reactions on single particles. In contrast to ESPR current imaging (Fig. 1), the signals were thought to originate from electron density changes. This is plausible because of fundamental differences between surface plasmons and nanoparticle plasmons, but it seems reasonable that both effects would contribute in both systems at least to some extent. Another application that has been suggested is intensity modulation through electrical control [86]. However, it seems difficult to get high enough intensity changes in response to a potential change, at least if the device is to be remain stable and not suffer any irreversible effects (Table 1). Wang and Lin [100] implemented electro-optical modulation in terms of frequency for plasmonic biosensing with gold nanoparticles and suggested this may improve the stability of the measurements.

An EIS–plasmonic biosensor for detection of peptides that form pores in membranes was demonstrated by Hiep et al. [101]. In this work, an artificial lipid membrane was formed by functionalizing silica particles coated with a continuous gold film (Fig. 4). EIS was used to detect membrane resistance changes while the plasmonic signal responded to protein accumulation in the membrane. In general, EIS is preferable for probing the intactness of artificial cell membranes [102] as it is highly sensitive also to single pore formation, especially at low frequencies (essentially DC). However, the plasmonic response becomes preferable at high pore densities since it scales linearly with the amount of bound protein (Fig. 4, graph A). The two techniques thus complement each other in dynamic range.

We recently demonstrated how to monitor electrochemical recrystallization of common vacuum-deposited metals through plasmon resonances [42]. It is very important to be aware of this effect when using any electrochemical–plasmonic device and thermal annealing is likely suitable as a final step in fabrication [93]. Plasmon resonances in gold nanodisks (and nanoholes) were used to monitor crystal grain growth in real time, as shown in Fig. 5. The initial and final full spectra are shown together with the optical monitoring of the crystallization process. The plasmon wavelength changes directly in response to switching the potential between −200 mV and +500 mV against Ag/AgCl, accompanied by a slow irreversible signal from grain growth. Importantly, when electrochemical crystallization was performed, the shape of the nanostructure was preserved so that the influence of crystallinity on plasmon resonances could be investigated independently. The spectral changes caused by changes in the free-electron properties were in excellent agreement with

Fig. 4 Detection of mellitin by a lipid membrane on plasmonic nanoparticles (*top*) probed by electrochemical impedance spectroscopy (**a**) and plasmonics (**b**). As melittin-induced pores start to form in the membrane, the resistance to charge transfer reactions decreases dramatically. The plasmonic signal has problems detecting low numbers of pores but can distinguish between high concentrations of melittin, in contrast to electrochemical impedance spectroscopy. *HBM* hybrid bilayer membrane. (Reprinted with permission from Hiep et al. [101]. Copyright 2008 American Chemical Society)
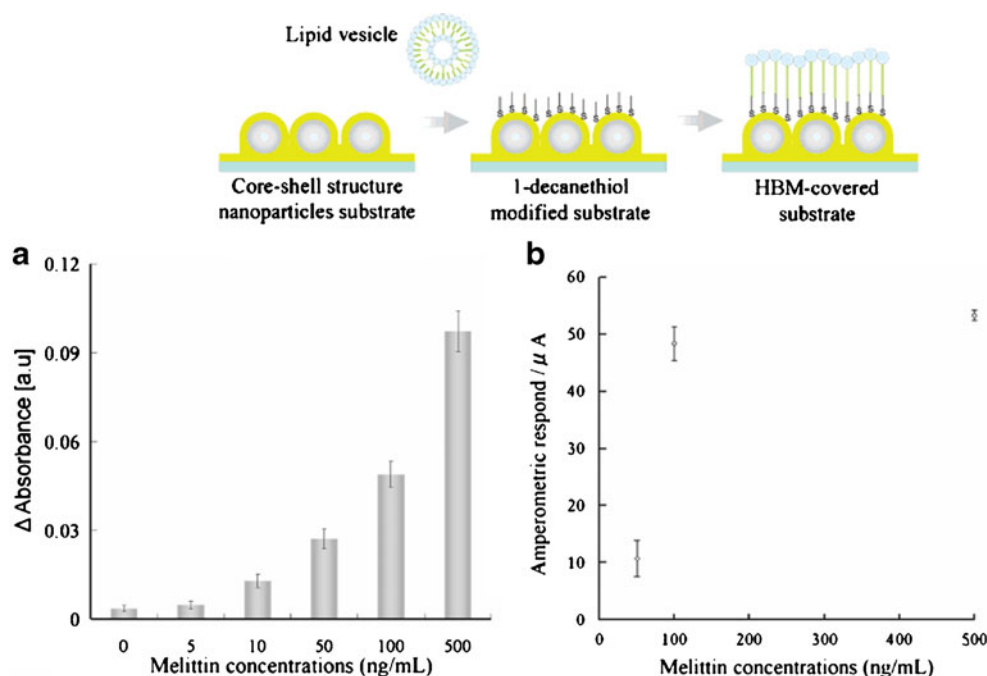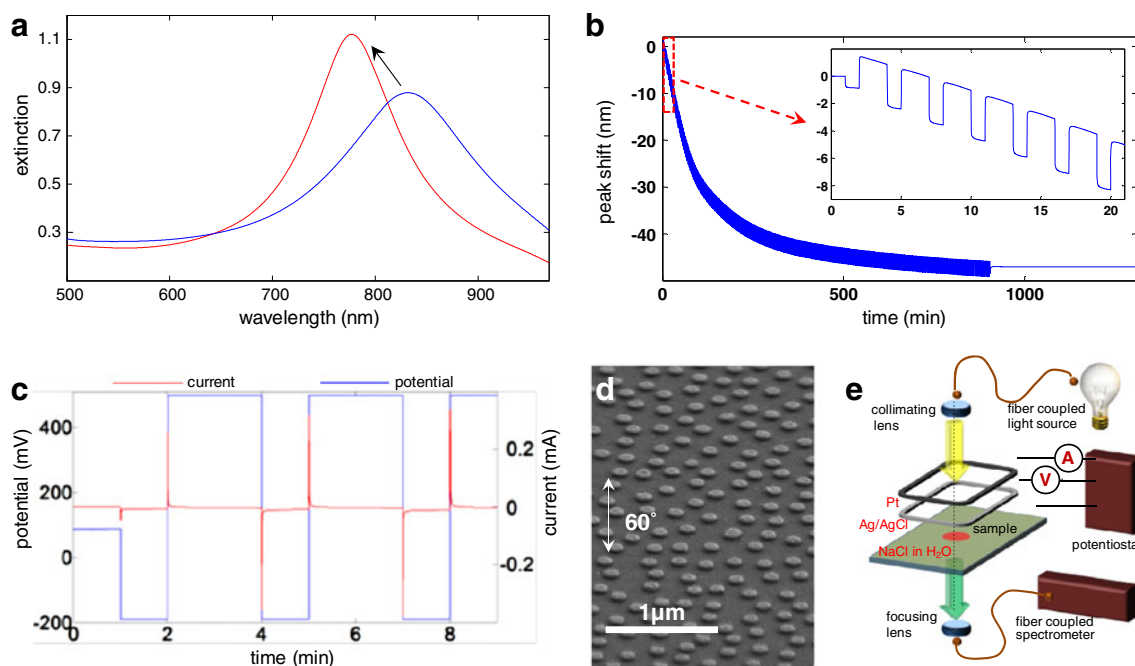
Fig. 5 Electrochemical crystallization of gold nanodisks. The spectrum in air before and after crystallization is shown in **a**. The peak shift (**b**) is monitored upon the application of capacitive electrochemical pulses (**c**), resulting in slow irreversible spectral changes in addition to the faster response from switching the potential. An electron microscopy image of nanodisks is shown in **d** and the experimental setup is shown in **e**. (Reprinted with permission from Dahlin et al. [42]. Copyright 2011 American Chemical Society)

analytical theory based on the Drude model. Similar results for metamaterials were obtained independently by Ruther et al. [103, 104].

Nanowire arrays

Fabrication of metallic nanowires has recently been of great interest owing to their unique optical and electrical properties [105–110]. Interestingly, nanowires support two very different types of plasmon resonances. Surface plasmons can propagate along the wire in a manner similar to "1D SPR", although this type of dispersed mode is of interest primarily for plasmonic waveguides rather than sensing [111]. The other type of mode is semilocalized or 2D *transverse* plasmons, which behave essentially identically to nanoparticle plasmons. The transverse dipoles are oriented perpendicular to the wire axis with coupling effects occurring in arrays of wires [106, 110, 112, 113]. In addition, the angle of incidence [114] and the cross-section shape [106, 115] influence the resonance. The refractometric sensing properties of the transverse plasmons in nanowires are similar to those of metal nanoparticles when compared in terms of resonance wavelength sensitivity, e.g. 17 nm [115] or 104 nm [106] per RI increment. The field around the wires can be strongly confined with simulated decay lengths of approximately 5 nm [116].

For electrical measurements, the nanowire geometry has the additional advantage of a conducting path along the wire [33, 34]. It is known that the electrical resistance in metal nanowires is much higher than what is expected from the bulk resistivity of the metal because of scattering of electrons at the *surface*. This phenomenon becomes relevant if at least one dimension is comparable to or smaller than the Drude electron mean free path (38 nm in gold) [45] and has an optical analogy in the additional plasmon damping in nanoparticles of very small size (less than 10 nm) [77]. In addition, electron scattering at crystal *grain boundaries* can contribute greatly to the resistance [117]. This is in analogy to the optical effects of crystallization in gold (Fig. 5). Interestingly, the influence of grain boundary scattering depends strongly on how the wires are fabricated [109]. For sensor applications, the resistance in the wire should preferably be dominated by surface scattering, in which case porous wires can be of interest [118].

In terms of chemical sensing, there are various reports on conductivity changes due to alkanethiol monolayer formation on gold wires [107, 109, 118], which typically results in relative resistance changes between 1% and 10%. The signal depends strongly on the strength and chemical nature of the molecular interaction with the metal [55]. This type of conductivity measurement will likely provide important information on interface phenomena although it remains unclear if it has value in, for instance, biosensing with a proper recognition interface [20]. So far, there have been no measurements of biomolecular interactions by conductivity

measurements in metallic nanowires. We have recently studied gold nanowire arrays fabricated by extreme UV interference lithography [105, 116, 119] for sensing applications with combined optical and electrical detection. Figure 6 shows a basic characterization of the plasmonic response (resonance wavelength) to electrochemical potentials over the whole array. We are currently extending this system to conductivity measurements along the wires (R. MacKenzie, C. Fraschina, B. Dielacher, T. Sannomiya, A. B. Dahlin, J. Vörös, unpublished work), which may help elucidate which effects from Table 1 dominate the spectral changes, such as those in Fig. 6.

Notably, the nanowire arrays such as those in Fig. 6 are very similar to interdigitated electrodes, which are commonly used for EIS [39]. It should therefore be straightforward to implement optical detection based on transverse wire plasmons together with EIS. Indeed, much of the literature on EIS claims that the *geometry* of the system is highly important for good performance, which has led to the development of electrodes with a "nanogap" [120] or 3D configuration [121]. Notably, there is a great variation in the LOD in EIS reports [40] with values down to 1 fM [41], but detection from real biological samples is rarely performed [122], especially when the LOD is defined [39]. Also, there is no consensus on whether the presence of charge transfer species is needed in the solution to enhance the faradaic response [120, 123]. In addition, some articles have reported the use of a standard three-electrode setup for EIS sensing, showing impressive LODs in complex biological samples [122] without any special properties of the gold working electrode. This suggests that interdigitated wirelike electrodes are not a necessity and that it is possible to combine plasmonic and EIS sensing for all the geometries discussed here.

Nanoholes in metal films

Nanoholes, typically around 100 nm in diameter, in metal films can be prepared by colloidal lithography [124, 125], focused ion beam [126] or interference lithography [127]. The peculiar optical properties of nanohole arrays [128], which were first observed by Ebbesen et al. [129], are complex owing to the presence of both localized and propagating plasmons as well as their interaction effects [130]. Analytical theory is limited to hypothetical "perfect conductors" and not Drude-like metals [131]. Still, the spectral features can be qualitatively understood fairly well and even predicted with decent accuracy for both long-range and short- range order [126] (Fig. 7a). The extinction spectrum of nanoholes in thin (up to 50 nm) films contains one peak (transmission minimum) corresponding to grating-coupling SPR [11] for the bonding mode [132] accompanied by a minimum (enhanced transmission) at a nearby longer wavelength. This represents a localized void resonance. Despite the complexity of the optical properties of nanohole arrays their refractometric sensing properties are very similar to those of nanoparticles [125]. The LOD in terms of RI for nanohole arrays in gold is typically between 10^{-5} and 10^{-6} in optimized setups [133] and the sensitivity is quite localized to the surface (less than 100 nm) [22].

Nanohole arrays are readily compatible with electrical detection principles because the continuous metal film acts as a conductive electrode [22]. Although refractometric

Fig. 6 Optical response upon applying an electrochemical potential to a gold nanowire array. The plasmon resonance wavelength is monitored upon application of potential pulses. Results are shown for two different nanowire array dimensions. (Reproduced from MacKenzie et al. [116])
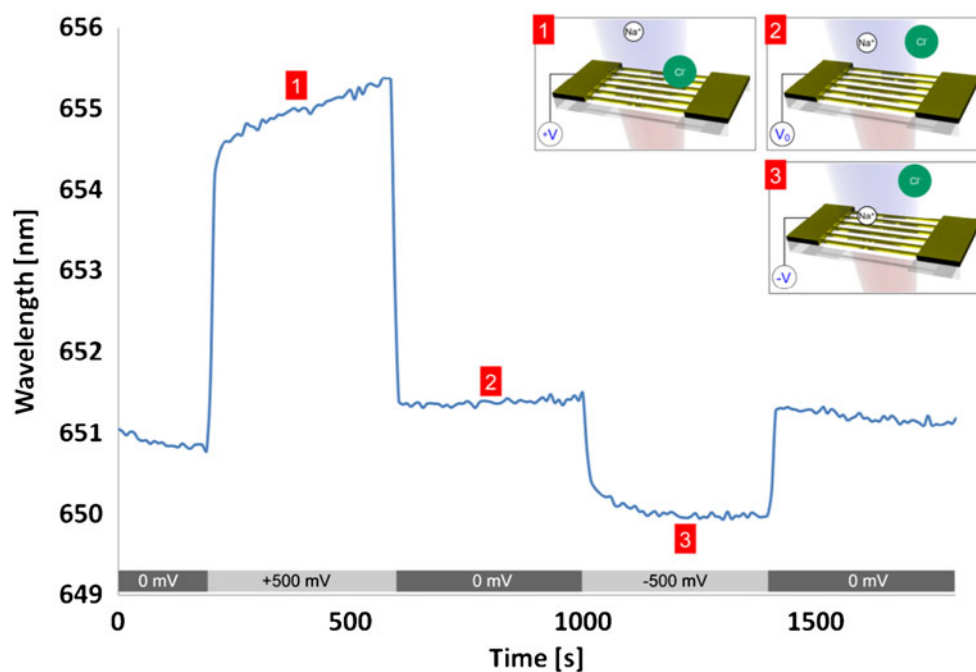
Fig. 7 Atomic force microscopy image of short-range ordered nanoholes in a silver film prepared by colloidal lithography (**a**). The conductivity of such silver films was studied for different numbers of holes in the film ("hole coverage" equals fractional area coverage) as shown in **b**. The fitted curve originates from percolation theory. (Reprinted with permission from Reilly et al. [138]. Copyright 2010 American Chemical Society)
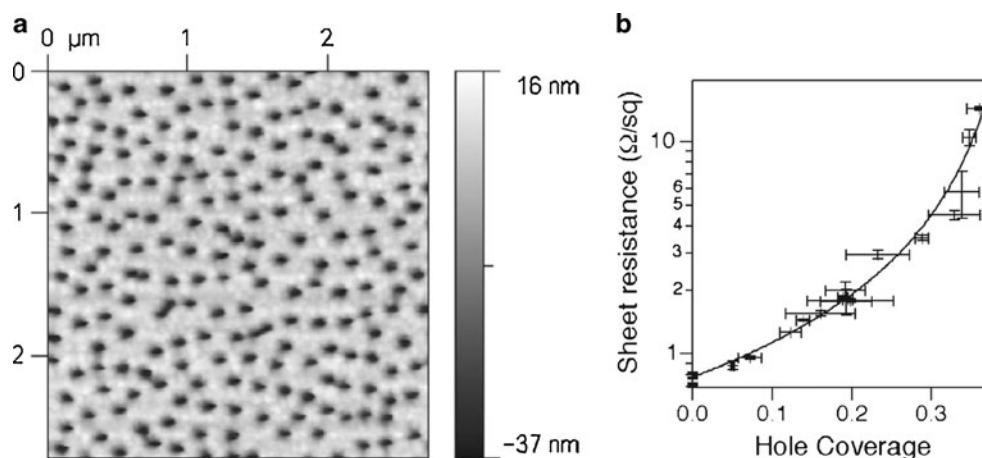
sensing with nanoholes has become very popular [16, 125], there are so far hardly any reports on the implementation of electrical measurements. The spectral response of the extinction peak due to applied potentials is more complicated to model [42] regardless of which one of the effects in Table 1 is considered. In response to positive potentials the peak red-shifts and broadens, indicating lower surface plasmon energy and lifetime [42]. This effect can be quantitatively modelled by considering the resonance as a geometrical effect, i.e. the resonance *wavevector* of the surface plasmon is determined by the periodicity. For single hole resonances [134], the *diameter* determines the wavevector in a similar manner [132]. One would therefore expect the same wavevector also when the metal is under the influence of an electrochemical potential, but a different resonance frequency [42]. Indeed, the dispersion relation of the surface plasmons will change and the resonance shift can be calculated by modifying the dispersion relation accordingly [42], assuming that the presence of holes simply introduces a constant offset error [126]. It would then be possible to introduce a surface layer describing the electric double-layer capacitor and then solve the dispersion relation for a multilayer system [135].

As discussed for nanowires, it is sufficient that a metal structure has at least one dimension comparable to the mean free path of conduction electrons for surface scattering of electrons to influence conductivity. However, other factors contribute as well [136, 137] and a deeper understanding of exactly how the electron movement contributes to the resistance is needed [45]. In any case, nanohole arrays offer a nice way to implement thin-film conductivity measurements [136, 137] synchronized with plasmonic sensing. Preliminary work on how the presence of holes influences film resistivity has been performed by Reilly et al. [138], as shown in Fig. 7. The films were well described by percolation theory and the influence of holes depends on the structure dimensions in relation to the mean free path of electrons.

It is not straightforward to see why nanoholes would present any advantages over the other systems described above for combined plasmonic–electrochemical sensing. In general, the advantages of using nanoholes lie in the *geometry* of the structure. For one thing, nanoholes open up for liquid flow through the surface [139], which improves the binding rate by preventing depletion from slow diffusion. In addition, size-exclusion effects can be utilized to control if and how many entities enter a hole [14], making the surface act as a filter. It is also interesting to think of the possibilities of performing electrochemistry and plasmonic sensing [134] on molecules captured within individual holes.

Conclusions and outlook

After reviewing the recent advances in metallic nanostructures for combined electrical and optical signal transduction we wish to emphasize Table 1, which summarizes all possible effects on the plasmon resonances in response to electrochemical potentials. It is meant to act as a checklist for any researcher working with electrochemistry and plasmonics. Table 1 illustrates that it is not straightforward to understand how the implementation of electrical control influences the plasmonic sensor. Indeed, when browsing the literature one can observe several inconsistencies in how experimental results are interpreted in combined electrochemical–plasmonic systems. Most reports consider only one, possibly two, but sometimes even none of the points in Table 1 to explain the experimental results.

For the rest of this review, we wish to point out some more promising aspects of combined electrical and optical detection. We focus now on advantages that have not been realized yet and that are more speculative in nature. We first note that synchronized combinations of different signal transduction mechanisms generally tend to provide new

insights about the methods themselves [22, 92]. In particular, plasmonic readout should help elucidate the mysteries associated with EIS sensing mentioned above. Combinations may also help to improve the quantitative interpretation of a sensor response [22].

In addition, the plasmonic signal from refractometric detection (not SERS) is expected to be associated with a larger (although still very small) probing volume than conductivity measurements relying on electron surface scattering, which primarily senses molecules directly on the metal. Using these two detection concepts in combination should provide information about to what extent binding molecules are in direct contact with the metal. One could therefore use the combined method to distinguish interactions with a receptor on the surface from those directly with the metal. This naturally relates to the topic of non-specific binding in surface-based sensors.

Another advantage is that optical and electrical methods complement each other well when it comes to the size of the analyte. Refractometric detection of small molecules is challenging [24] and often requires competitive assays [141], but it is possible with SERS. In contrast, electrical detection through voltammetry can detect anything that participates in redox reactions. This also means that optical readout, given that the resolution is sufficient, should be able to be utilized for distinguishing if a redox-active species remains bound to the surface.

Electrochemistry may also contribute to another aspect of sensor design, namely chemical functionalization. As mentioned in "Introduction", specificity is critical for actually realizing the LOD associated with a physical transduction principle, and this aspect is sometimes overlooked when new sensors are presented. We note that electrochemistry offers new tools for controlling molecular binding [142], even in array formats [122, 143]. Therefore, incorporating electrochemistry may lead to improvement of surface functionalization strategies for optical sensors. In particular, electrochemistry easily offers specific functionalization of nanoscale regions [144], which should be highly useable for miniaturized sensors [145]. For instance, single nanoparticle plasmonic sensors have an extremely small sensing volume [18], but in the device binding may occur on a much larger area than that of the particle. This means that even if the measured signal originates from very few molecules, it would not be possible to detect so few molecules in a sample as they would end up binding at other locations.

A final and highly speculative advantage of electrochemistry for plasmonic sensors is to attract molecules to the sensor surface in order to overcome the performance limits set by mass transport limitations [13]. As long as the analyte carries a charge it will have an electrophoretic mobility which can be utilized to accumulate molecules at the surface [146]. Interestingly, the molecules could then be attracted to pointy structures in gold, where the field and the plasmonic sensitivity are both expected to be highest.

References

1. Drude P (1900) Ann Phys Berl 1566–613
2. Rapp BE, Gruhl FJ, Lange K (2010) Anal Bioanal Chem 398:2403–2412
3. Lee S-W, Lee K-S, Ahn J, Lee J-J, Kim M-G, Shin Y-B (2011) ACS Nano 5:897–904
4. Lyon LA, Musick MD, Natan MJ (1998) Anal Chem 70:5177–5183
5. Ramanathan K, Danielsson B (2001) Biosens Bioelectron 16:417–423
6. Chemla YR, Crossman HL, Poon Y, McDermott R, Stevens R, Alper MD, Clarke J (2000) Proc Natl Acad Sci USA 97:14268–14272
7. Janshoff A, Galla HJ, Steinem C (2000) Angew Chem Int Ed 39:4004–4032
8. Lange K, Rapp BE, Rapp M (2008) Anal Bioanal Chem 391:1509–1519
9. Hwang KS, Lee SM, Kim SK, Lee JH, Kim TS (2009) Annu Rev Anal Chem 2:77–98
10. Gauglitz G (2005) Anal Bioanal Chem 381:141–155
11. Homola J (2008) Chem Rev 108:462–493
12. Homola J (2003) Anal Bioanal Chem 377:528–539
13. Squires TM, Messinger RJ, Manalis SR (2008) Nat Biotechnol 26:417–426
14. Dahlin AB, Jonsson MP, Hook F (2008) Adv Mater 20:1436
15. Marinakos SM, Chen SH, Chilkoti A (2007) Anal Chem 79:5278–5283
16. Stewart ME, Anderton CR, Thompson LB, Maria J, Gray SK, Rogers JA, Nuzzo RG (2008) Chem Rev 108:494–521
17. Mayer KM, Hafner JH (2011) Chem Rev 111:3828–3857
18. Sannomiya T, Vörös J (2011) Trends Biotechnol 29:343–351
19. Anker JN, Hall WP, Lyandres O, Shah NC, Zhao J, Van Duyne RP (2008) Nat Mater 7:442–453
20. Bendikov TA, Rabinkov A, Karakouz T, Vaskevich A, Rubinstein I (2008) Anal Chem 80:7487–7498
21. Kedem O, Tesler AB, Vaskevich A, Rubinstein I (2011) ACS Nano 5:748–760
22. Dahlin AB, Jonsson P, Jonsson MP, Schmid E, Zhou Y, Hook F (2008) ACS Nano 2:2174–2182
23. Verellen N, Van Dorpe P, Huang C, Lodewijks K, Vandenbosch GAE, Lagae L, Moshchalkov VV (2011) Nano Lett 11:391–397
24. Kabashin AV, Evans P, Pastkovsky S, Hendren W, Wurtz GA, Atkinson R, Pollard R, Podolskiy VA, Zayats AV (2009) Nat Mater 8:867–871
25. Elghanian R, Storhoff JJ, Mucic RC, Letsinger RL, Mirkin CA (1997) Science 277:1078–1081
26. Laromaine A, Koh LL, Murugesan M, Ulijn RV, Stevens MM (2007) J Am Chem Soc 129:4156
27. Liu GL, Yin YD, Kunchakarra S, Mukherjee B, Gerion D, Jett SD, Bear DG, Gray JW, Alivisatos AP, Lee LP, Chen FQF (2006) Nat Nanotechnol 1:47–52
28. Reinhard BM, Sheikholeslami S, Mastroianni A, Alivisatos AP, Liphardt J (2007) Proc Natl Acad Sci USA 104:2667–2672
29. Sonnichsen C, Reinhard BM, Liphardt J, Alivisatos AP (2005) Nat Biotechnol 23:741–745
30. Giljohann DA, Seferos DS, Daniel WL, Massich MD, Patel PC, Mirkin CA (2010) Angew Chem Int Ed 49:3280–3294
31. Alvarez-Puebla RA, Liz-Marzan LM (2010) Small 6:604–610
32. Makowski MS, Ivanisevic A (2011) Small 7:1863–1875

33. Cui Y, Wei QQ, Park HK, Lieber CM (2001) Science 293:1289–1292
34. Zheng GF, Patolsky F, Cui Y, Wang WU, Lieber CM (2005) Nat Biotechnol 23:1294–1301
35. Grieshaber D, MacKenzie R, Voros J, Reimhult E (2008) Sensors 8:1400–1458
36. Baba A, Taranekar P, Ponnapati RR, Knoll W, Advincula RC (2010) ACS Appl Mater Interfaces 2:2347–2354
37. Goluch ED, Wolfrum B, Singh PS, Zevenbergen MAG, Lemay SG (2009) Anal Bioanal Chem 394:447–456
38. Zachek MK, Park J, Takmakov P, Wightman RM, McCarty GS (2010) Analyst 135:1556–1563
39. Lisdat F, Schafer D (2008) Anal Bioanal Chem 391:1555–1567
40. Daniels JS, Pourmand N (2007) Electroanalysis 19:1239–1257
41. Berggren C, Bjarnason B, Johansson G (2001) Electroanalysis 13:173–180
42. Dahlin AB, Sannomiya T, Zahn R, Sotiriou GA, Vörös J (2011) Nano Lett 11:1337–1343
43. Freestone I, Meeks N, Sax M, Higgitt C (2007) Gold Bull 40:270–277
44. Johnson PB, Christy RW (1972) Phys Rev B 6:4370–4379
45. Zhang W, Brongersma SH, Richard O, Brijs B, Palmans R, Froyen L, Maex K (2004) Microelectron Eng 76:146–152
46. Haes AJ, Van Duyne RP (2004) Anal Bioanal Chem 379:920–930
47. Liedberg B, Nylander C, Lundstrom I (1983) Sens Actuators 4:299–304
48. Chan GH, Zhao J, Hicks EM, Schatz GC, Van Duyne RP (2007) Nano Lett 7:1947–1952
49. Gao H, Henzie J, Lee MH, Odom TW (2008) Proc Natl Acad Sci USA 105:20146–20151
50. Langhammer C, Yuan Z, Zoric I, Kasemo B (2006) Nano Lett 6:833–838
51. Vestergaard MD, Kerman K, Tamiya E (2007) Sensors 7:3442–3458
52. Zhang N, Schweiss R, Zong Y, Knoll W (2007) Electrochim Acta 52:2869–2875
53. Abeles F, Lopezrios T, Tadjeddine A (1975) Solid State Commun 16:843–847
54. Shan XN, Patel U, Wang SP, Iglesias R, Tao NJ (2010) Science 327:1363–1366
55. Zhang YM, Terrill RH, Bohn PW (1999) Anal Chem 71:119–125
56. Xia C, Advincula RC, Baba A, Knoll W (2002) Langmuir 18:3555–3560
57. Wang YJ, Knoll W (2006) Anal Chim Acta 558:150–157
58. Kang XF, Cheng GJ, Dong SJ (2001) Electrochem Commun 3:489–493
59. Baba A, Advincula RC, Knoll W (2002) J Phys Chem B 106:1581–1587
60. Hanken DG, Corn RM (1997) Anal Chem 69:3665–3673
61. McIntyre JD (1973) Surf Sci 37:658–682
62. Tadjeddine A, Kolb DM, Kotz R (1980) Surf Sci 101:277–285
63. Iwasaki Y, Horiuchi T, Morita M, Niwa O (1998) Sens Actuators B Chem 50:145–148
64. Foley KJ, Shan X, Tao NJ (2008) Anal Chem 80:5146–5151
65. Kolb DM (2001) Angew Chem Int Ed 40:1162–1181
66. Wang S, Huang X, Shan X, Foley KJ, Tao N (2010) Anal Chem 82:935–941
67. Scarano S, Mascini M, Turner APF, Minunni M (2010) Biosens Bioelectron 25:957–966
68. Grzelczak M, Perez-Juste J, Mulvaney P, Liz-Marzan LM (2008) Chem Soc Rev 37:1783–1791
69. Kim F, Connor S, Song H, Kuykendall T, Yang PD (2004) Angew Chem Int Ed 43:3673–3677
70. Wang H, Brandl DW, Nordlander P, Halas NJ (2007) Acc Chem Res 40:53–62
71. Hanarp P, Kall M, Sutherland DS (2003) J Phys Chem B 107:5768–5772
72. Haynes CL, Van Duyne RP (2001) J Phys Chem B 105:5599–5611
73. Aizpurua J, Hanarp P, Sutherland DS, Kall M, Bryant GW, de Abajo FJG (2003) Phys Rev Lett 90:057401
74. Bukasov R, Shumaker-Parry JS (2007) Nano Lett 7:1113–1118
75. Takei H, Himmelhaus M, Okamoto T (2002) Opt Lett 27:342–344
76. Heo CJ, Kim SH, Jang SG, Lee SY, Yang SM (2009) Adv Mater 21:1726–1731
77. Myroshnychenko V, Rodriguez-Fernandez J, Pastoriza-Santos I, Funston AM, Novo C, Mulvaney P, Liz-Marzan LM, de Abajo FJG (2008) Chem Soc Rev 37:1792–1805
78. Kelly KL, Coronado E, Zhao LL, Schatz GC (2003) J Phys Chem B 107:668–677
79. Englebienne P (1998) Analyst 123:1599–1603
80. Daniel MC, Astruc D (2004) Chem Rev 104:293–346
81. Shipway AN, Lahav M, Willner I (2000) Adv Mater 12:993–998
82. Mulvaney P (1996) Langmuir 12:788–800
83. Murray RW, Templeton AC, Pietron JJ, Mulvaney P (2000) J Phys Chem B 104:564–570
84. Ung T, Giersig M, Dunstan D, Mulvaney P (1997) Langmuir 13:1773–1782
85. Oldfield G, Ung T, Mulvaney P (2000) Adv Mater 12:1519–1522
86. Chapman R, Mulvaney P (2001) Chem Phys Lett 349:358–362
87. Miyazaki T, Hasegawa R, Yamaguchi H, Oh-Oka H, Nagato H, Amemiya I, Uchikoga S (2009) J Phys Chem C 113:8484–8490
88. Novo C, Funston AM, Gooding AK, Mulvaney P (2009) J Am Chem Soc 131:14664–14666
89. Novo C, Funston AM, Mulvaney P (2008) Nat Nanotechnol 3:598–602
90. Novo C, Mulvaney P (2007) Nano Lett 7:520–524
91. Qu XH, Peng ZQ, Jiang X, Dong SJ (2004) Langmuir 20:2519–2522
92. Sannomiya T, Dermutz H, Hafner C, Voros J, Dahlin AB (2010) Langmuir 26:7619–7626
93. Szunerits S, Praig VG, Manesse M, Boukherroub R (2008) Gold island films on indium tin oxide for localized surface plasmon sensing. Nanotechnology 19:195712
94. Zhang X, Hicks EM, Zhao J, Schatz GC, Van Duyne RP (2005) Nano Lett 5:1503–1507
95. Kanehara M, Koike H, Yoshinaga T, Teranishi T (2009) J Am Chem Soc 131:17736–17737
96. Armstrong NR, Lin AWC, Fujihira M, Kuwana T (1976) Anal Chem 48:741–750
97. Loo BH (1982) J Phys Chem 86:433–437
98. Ivanova OS, Zamborini FP (2009) J Am Chem Soc 132:70–72
99. Gao P, Weaver MJ (1986) J Phys Chem 90:4057–4063
100. Wang TJ, Lin WS (2006) Appl Phys Lett 89:173903
101. Hiep HM, Endo T, Saito M, Chikae M, Kim DK, Yamamura S, Takamura Y, Tamiya E (2008) Anal Chem 80:1859–1864
102. Janshoff A, Steinem C (2006) Anal Bioanal Chem 385:433–451
103. Ruther M, Shao L-H, Linden S, Weissmüller J, Wegener M (2011) Appl Phys Lett 98:013112
104. Shao L-H, Ruther M, Linden S, Essig S, Busch K, Weissmüller J, Wegener M (2010) Adv Mater 22:5173–5177
105. Auzelyte V, Solak HH, Ekinci Y, MacKenzie R, Voros J, Olliges S, Spolenak R (2008) Microelectron Eng 85:1131–1134
106. Chen HA, Lin HY, Lin HN (2010) J Phys Chem C 114:10359–10364
107. Lin HY, Chen HA, Lin HN (2008) Anal Chem 80:1937–1941
108. Menke EJ, Thompson MA, Xiang C, Yang LC, Penner RM (2006) Nat Mater 5:914–919
109. Shi P, Zhang JY, Lin HY, Bohn PW (2010) Small 6:2598–2603

110. Xu QB, Bao JM, Capasso F, Whitesides GM (2006) Angew Chem Int Ed 45:3631–3635

111. Lal S, Link S, Halas NJ (2007) Nat Photonics 1:641–648

112. Schider G, Krenn JR, Gotschy W, Lamprecht B, Ditlbacher H, Leitner A, Aussenegg FR (2001) J Appl Phys 90:3825–3830

113. Della Valle G, Sondergaard T, Bozhevolnyi SI (2008) Opt Express 16:6867–6876

114. Sosnova MV, Dmitruk NL, Korovin AV, Mamykin SV, Mynko VI, Lytvyn OS (2010) Appl Phys B Lasers Opt 99:493–497

115. Byun KM, Kim SJ, Kim D (2006) Appl Opt 45:3382–3389

116. MacKenzie R, Fraschina C, Sannomiya T, Auzelyte V, Vörös J (2010) Sensors 10:9808–9830

117. Durkan C, Welland ME (2000) Phys Rev B 61:14215–14218

118. Liu Z, Searson PC (2006) J Phys Chem B 110:4318–4322

119. MacKenzie R, Fraschina C, Sannomiya T, Voros J (2011) Nanotechnology 22:055203

120. Singh KV, Whited AM, Ragineni Y, Barrett TW, King J, Solanki R (2010) Anal Bioanal Chem 397:1493–1502

121. Bratov A, Ramon-Azcon J, Abramova N, Merlos A, Adrian J, Sanchez-Baeza F, Marco MP, Dominguez C (2008) Biosens Bioelectron 24:729–735

122. Evans D, Johnson S, Laurenson S, Davies AG, Ko Ferrigno P, Walti C (2008) J Biol 7:3

123. Hou YX, Helali S, Zhang AD, Jaffrezic-Renault N, Martelet C, Minic J, Gorojankina T, Persuy MA, Pajot-Augy E, Salesse R, Bessueille F, Samitier J, Errachid A, Akimov V, Reggiani L, Pennetta C, Alfinito E (2006) Biosens Bioelectron 21:1393–1402

124. Prikulis J, Hanarp P, Olofsson L, Sutherland D, Kall M (2004) Nano Lett 4:1003–1007

125. Jonsson MP, Dahlin AB, Jonsson P, Hook F (2008) Biointerphases 3:FD30–FD40

126. Sannomiya T, Scholder O, Jefimovs K, Hafner C, Dahlin AB (2011) Small 7:1653–1663

127. Henzie J, Lee MH, Odom TW (2007) Nat Nanotechnol 2:549–554

128. Genet C, Ebbesen TW (2007) Nature 445:39–46

129. Ebbesen TW, Lezec HJ, Ghaemi HF, Thio T, Wolff PA (1998) Nature 391:667–669

130. Garcia-Vidal FJ, Martin-Moreno L, Ebbesen TW, Kuipers L (2010) Rev Mod Phys 82:729–787

131. de Abajo FJG (2007) Rev Mod Phys 79:1267–1290

132. Park TH, Mirin N, Lassiter JB, Nehl CL, Halas NJ, Nordlander P (2008) ACS Nano 2:25–32

133. Dahlin AB, Tegenfeldt JO, Hook F (2006) Anal Chem 78:4416–4423

134. Rindzevicius T, Alaverdyan Y, Dahlin A, Höök F, Sutherland DS, Käll M (2005) Nano Lett 5:2335–2339

135. Ward CA, Bhasin K, Bell RJ, Alexander RW, Tyler I (1975) J Chem Phys 62:1674–1676

136. Tobin RG (2002) Surf Sci 502:374–387

137. Tucceri R (2004) Surf Sci Rep 56:85–157

138. Reilly TH, Tenent RC, Barnes TM, Rowlen KL, van de Lagemaat J (2010) ACS Nano 4:615–624

139. Jonsson MP, Dahlin AB, Feuz L, Petronis S, Hook F (2010) Anal Chem 82:2087–2094

140. Moreira CS, Lima AMN, Neff H, Thirstrup C (2008) Sens Actuators B 134:854–862

141. Mitchell JS, Wu YQ, Cook CJ, Main L (2005) Anal Biochem 343:125–135

142. Liron Z, Tender LM, Golden JP, Ligler FS (2002) Biosens Bioelectron 17:489–494

143. Tang CS, Dusseiller M, Makohliso S, Heuschkel M, Sharma S, Keller B, Voros J (2006) Anal Chem 78:711–717

144. Walti C, Wirtz R, Germishuizen WA, Bailey DMD, Pepper M, Middelberg APJ, Davies AG (2003) Langmuir 19:981–984

145. Beeram SR, Zamborini FP (2009) J Am Chem Soc 131:11689–11691

146. Heller MJ, Forster AH, Tu E (2000) Electrophoresis 21:157–164